

High-precision 3D Modeling of Construction Waste Pile Bodies by Integrating Multi-source Data

Leyan Shi ¹, Wenji Zhao ¹, Yanhui Wang ¹, Xing Yan ²

¹ College of Resource Environment and Tourism, Capital Normal University, Beijing, China – 2230902199@cnu.edu.cn;
4973@cnu.edu.cn; yanhuiwang@cnu.edu.cn

² State Key Laboratory of Remote Sensing Science Faculty of Geographical Science, Beijing Normal University, Beijing, China -
yanxing@bnu.edu.cn

Keywords: Construction Waste Pile Bodies, Unmanned Aerial Vehicle Oblique Photography; Laser Point Cloud, Fine Three-dimensional Reconstruction, Data Fusion.

Abstract

The instability of construction waste pile bodies, as an increasingly concerning disaster, poses significant risks to the safety of people's lives and property. Currently, there is limited research on high-precision 3D modeling techniques for construction waste pile bodies, which significantly hinders the accuracy and reliability of early detection and risk assessment of pile body instability. Therefore, constructing high-precision 3D models of construction waste pile bodies using multi-source data plays a crucial role in improving the accuracy and timeliness of early warning systems for pile body instability, offering significant theoretical research and practical application value. Building 3D models of construction waste pile bodies solely based on unmanned aerial vehicle (UAV) oblique photography data faces challenges, such as various degrees of data voids and insufficient model completeness, and few methods currently address the construction of 3D models of construction waste pile bodies through the fusion of multi-source data. This paper attempts to use the Iterative Closest Point (ICP) algorithm, combining SLAM laser point cloud data with UAV oblique photography data to fill data voids, and utilizes the fused point cloud to reconstruct the triangulation network, achieving the transformation from 3D point cloud models to 3D surface models. On the basis of texture mapping, a high-precision 3D model of the construction waste pile body is constructed. The research results show that the 3D model of the construction waste pile body, integrated with multi-source data, has a planar error of 0.0187m and an elevation error of 0.0368m, meeting the corresponding model accuracy requirements. It can more realistically restore the fine 3D features of the construction waste pile body, effectively compensating for the shortcomings of single-source data in 3D modeling of construction waste pile bodies, providing a new method for the 3D model reconstruction of construction waste pile bodies, and offering effective data support for construction waste research.

1. Introduction

According to the statistical data from (Sirimewan et al., 2024) and (Sivashanmugam et al., 2023), rapid urbanization has led to a significant amount of solid waste generated by construction activities worldwide, with approximately 35% of global solid waste being attributed to the construction industry. For instance, in the United States, the generation of construction and demolition waste (CDW) reached 534 million metric tons in 2016 (Guerra & Leite, 2021), accounting for 67% of the total solid waste (Wang et al., 2024). In the United Kingdom, CDW amounted to 138 million metric tons in 2018 (Petrović & Thomas, 2024), representing 62% of the total solid waste (Segara et al., 2024). Germany produced 230.9 million metric tons of CDW in 2019, accounting for 55.4% of the total waste production (Liang et al., 2024). In China, demolition of existing buildings and new construction contribute to 30% to 40% of urban solid waste (Liu et al., 2023). According to (Li et al., 2022), on average, every 10,000 square meters of building area generates 550 tons of construction waste, accounting for 35% of urban construction waste. Currently, landfilling is the most efficient and cost-effective method for disposing of construction waste. However, in practice, in order to handle larger volumes, construction waste piles often approach the critical threshold of instability. Under external influences, this can lead to slope failures, landslides, and collapses, resulting in severe casualties and environmental pollution. Timely monitoring of construction waste piles is crucial for their safe management. Presently, the deformation monitoring methods for construction waste piles

mainly rely on manual field inspections and remote sensing techniques. The distribution of construction waste piles is uneven, irregular in quantity, and complex in scope, making field surveys resource-intensive and inefficient. In recent years, traditional surveying has transitioned from two-dimensional to three-dimensional, spurring the development of various three-dimensional remote sensing monitoring methods, such as aerospace and ground laser scanning. Three-dimensional models can greatly restore the true surface conditions, providing a data foundation for achieving comprehensive digital monitoring of construction waste piles.

UAV oblique photography enables the automatic and efficient acquisition of sub-centimeter to millimeter-scale remote sensing images through drones, thereby achieving detailed three-dimensional modeling of ground objects (He et al., 2024). (Onososen et al., 2023) proposed using UAV photogrammetry technology to overcome obstacles in the digitization of the built environment. (Forcael et al., 2023) demonstrated the use of UAV photography to capture digital images for the assessment of bridge cracks and fissures. In practical measurement processes, UAV oblique photography technology is susceptible to influences from terrain, climate, and other factors, and has limitations in modeling small objects.

Three-dimensional laser scanners can quickly obtain the three-dimensional coordinates of target points using laser ranging technology (LiDAR), characterized by high automation, high

resolution, and high accuracy. (Zhao et al., 2023) applied three-dimensional laser scanning technology to tunnel engineering, finding it more efficient and accurate than traditional methods for obtaining deformation results and spatial evolution conditions. (J.-w. Zhou et al., 2024) utilized ground laser scanning technology for the discontinuous automatic identification and quantitative monitoring of unstable landslide blocks, enabling the rapid and accurate acquisition of slope terrain and geological information. However, ground laser scanner results may suffer from significant point cloud noise, uneven density distribution, ghosting phenomena, and inaccurate synthesis of color information.

Both single data sources have their respective limitations. The most widely applied method for constructing high-precision 3D models currently involves the fusion of multiple data sources. Researchers both domestically and internationally employ various data acquisition methods and 3D modeling techniques, investigating refined reconstruction methods based on multi-source data. (Zeng et al., 2023) used oblique photogrammetry and vehicle-mounted laser point clouds as data sources in urban high-precision modeling, finding that fused data addressed issues of texture blurring and model deformation inherent in single data sources. By integrating UAV photogrammetry with 3D laser scanning, (Terryn et al., 2022) constructed detailed 3D models of forest structures. (Jo et al., 2024) obtained external images and internal point clouds of wooden pagodas, completing precision analysis for deformation monitoring. (Chen et al., 2024) building on the integration of both methods, used TIN matching algorithms to optimize and reconstruct the complete structure of forests. However, regarding the 3D modeling of construction waste piles, few studies have addressed how to unify LiDAR point clouds with UAV imagery coordinate systems, thereby resolving issues of data voids and model distortion caused by single data source modeling.

In summary, the current stage of refined 3D reconstruction based on multi-source data primarily achieves this through the combination of oblique photography and 3D laser scanning, mostly employing point-to-point matching fusion methods for detailed 3D model reconstruction. The research subjects mainly include vegetation and buildings, with few applications in the 3D modeling of construction waste piles. Addressing the limitations of current UAV oblique photogrammetry and LiDAR scanning modeling technologies, this paper proposes a 3D real-scene fusion modeling method based on the integration of these two technologies. First, UAV oblique photogrammetry is used to capture multi-angle high-resolution images. Second, laser point clouds are used to provide dense point clouds for extracting edge information of construction waste. Finally, the ICP (Iterative Closest Point) algorithm is employed for precise registration and model construction, transforming the fused point cloud from a point cloud model to a surface model. This method constructs the complete geometric shape and texture information of buildings, achieving refined 3D modeling of construction waste piles.

2. Data and Methods

2.1 Research Area

The construction waste pile is located within Zhuozhou City, Hebei Province. It stands approximately 30 meters high and covers an area of about 62,128.2 square meters. The disposal site is used for storing mixed waste, predominantly consisting of construction debris. It consists of a single main mound surrounded by protective fences. There is a single cement-

hardened road leading to the top of the mound. The surrounding area of the mound is farmland without any other interfering objects. However, the research indicates that there are small-scale collapses within the waste mound, and as the level of activity increases, there is a potential risk of instability in the mound. Therefore, the site exhibits good representativeness.

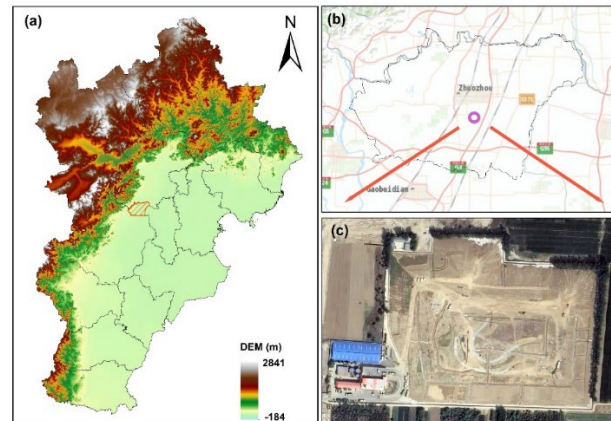


Figure 1. Overview of Construction Waste Piles

2.2 UAV Oblique Photography for 3D Modeling

To create a 3D model of the construction waste pile using UAV oblique photogrammetry, the collected images are first preprocessed to remove borders and correct distortions. Next, aerial triangulation is performed to ensure the accuracy and authenticity of the calculated results. Finally, the 3D modeling is completed using Context Capture software.

| model | parameter | indicator |
|--------|-----------------------------|---|
| Camera | Maximum resolution of image | 4864*3648 (4: 3) 5472*3648 (3: 2) |
| | Type of image | JPEG |
| GNSS | Satellite | GLONASS: L1/L2 BeiDou: B1/B2 Galileo: E1/E5 |
| | Positioning accuracy | Vertical 1.52cm+1ppm(RMS) horizontal 1cm+1ppm(RMS) |

Table 1. Parameters of the UAV

The internal data values of the construction waste pile region are extracted, with the exterior orientation elements of multi-view images provided by POS data serving as initial values. The SIFT (Scale-Invariant Feature Transform) algorithm is employed to extract and match overall point features. By identifying target objects in the images, tie points between images are obtained to complete the image matching process. The matched images are connected to the internal coordinate points of the experimental area using a free-network bundle adjustment method. Through adjustment calculations, multi-view image adjustment iterative calculations are achieved, resulting in densified point cloud data. Context Capture is selected as the 3D reconstruction software application. Using the overall image matching algorithm, images are matched based on feature points to establish links between different images. The generated point cloud data is then used to construct a TIN (Triangulated Irregular Network). The software calculates the texture corresponding to the model and maps it comprehensively to establish a white model mode with the TIN,

thus generating the 3D model of the construction waste pile. The parameters used during UAV flight are listed in Table 1.

2.3 3D Modeling Using Laser Point Clouds

For the acquired laser point cloud data, it is first necessary to preprocess the data, including steps such as point cloud denoising, stitching, and segmentation. This is to eliminate abnormal points caused by equipment errors or environmental factors, thereby improving the efficiency and accuracy of subsequent processing. Then, the SLAM algorithm is used for real-time motion estimation and data matching to efficiently obtain a 3D point cloud of the construction waste pile, ultimately completing the 3D reconstruction of the construction waste pile (Tysiac et al., 2023). The radar parameters we used are shown in Table 2.

| Devices | Main indicators | Parameters |
|---------------------------|---|------------|
| Laser scanner | Scanning frequency/Hz | 20 |
| | Scanning distance/m | 100 |
| | Scanning angle/deg | 360*30 |
| | Angular resolution/deg | 0.4 |
| | Wavelength/nm | 903 |
| | Stability of gyroscope | 0.5 |
| Inertial measurement unit | Angle drift | 0.15 |
| | Angular velocity input range | ±400 |
| | Temperature deviation error of Gyroscopic | 10 |
| | Accelerometer zero shift | 0.05 |
| | Acceleration input range | ±10 |
| Compute | CPU | i5 |
| | Memory/GB | 8 |
| | Disk/GB | 500 |

Table 2. Parameters of the Lidar

The SLAM algorithm is used to process the preprocessed point cloud data. SLAM optimizes iteratively to estimate the device's position and orientation and construct an environmental map. In each iteration, the algorithm predicts the next moment's point cloud data based on the current pose and matches it with the actually acquired point cloud data to estimate the device's motion trajectory and the geometric structure of the environment, thereby performing 3D reconstruction. By integrating point cloud data from different moments and perspectives, a 3D model of the target environment can be constructed. This 3D model includes information about the shape, position, and pose of objects in the environment, which can be used for subsequent analysis, visualization, and other applications. After the 3D reconstruction is completed, the model can be smoothed to reduce noise interference and texture information can be added to enhance the visual effect of the model, restoring the 3D shape of the pile itself.

2.4 Refined 3D Modeling Method Based on Multi-Source Data Using the ICP Algorithm

In practical operations, due to the scanning angle limitations of laser scanners, data loss may occur. Similarly, UAV aerial surveys may experience data loss due to obstructions like perimeter walls or excessive terrain tilt. Achieving precise monitoring of construction waste piles requires addressing data voids caused by single data sources. Common point cloud repair methods often struggle to produce satisfactory results for large-area data voids, and using the data itself to repair 3D data can only ensure the data approximates reality, but the accuracy of the

3D model remains significantly constrained. Therefore, this paper introduces the Iterative Closest Point (ICP) algorithm for data fusion to compensate for the shortcomings of both monitoring methods (Parente et al., 2021).

The ICP algorithm solves for the rotation matrix and translation matrix between two sets of point clouds (Li et al., 2023). The principle is to use one point cloud as the reference point cloud and establish the relationship between the corresponding points in the point cloud to be registered and the reference point cloud using the least squares method. This process completes the calculation of the rotation matrix and translation matrix. The ICP algorithm iteratively acquires the set of corresponding points, and the termination condition can be set based on an error threshold or the number of iterations.

If we denote the two sets of 3D point cloud data as point cloud data $A(a_1, a_2, \dots, a_n)$ and point cloud data (b_1, b_2, \dots, b_n) , where A contains N points that have corresponding points in B , we designate one set as the reference point cloud group, such as specifying A as the reference point cloud group. Then, we rotate and translate B to obtain the set of as many corresponding points N as possible. The formula is as follows:

$$E(R, T) = \frac{1}{N} \sum_{i=1}^n \|a_i - (Rb_i + T)\|^2 \quad (1)$$

Here, R is the rotation matrix, T is the translation vector, N is the number of nearest point pairs, a_i is a point in the target point cloud A , and b_i is the nearest corresponding point in the source point cloud B to a_i . Essentially, point cloud registration is about finding the minimum value of this expression.

To achieve the fusion of multi-source data, first, three-dimensional point cloud data based on drone oblique photography and SLAM lidar 3D modeling are acquired separately. Then, the ICP algorithm is introduced to complete the precise registration of point cloud data, unifying the point clouds obtained from the two data sources into the same coordinate system. Due to the alignment of the three-dimensional model of the building debris heap with its texture, this study uses the three-dimensional point cloud of drone oblique photography as the registration reference. The SLAM lidar point cloud data is registered to the drone point cloud, and after matching the point clouds, the registered point cloud can be overlaid and fused with the reference point cloud. At this point, a completely new fused point cloud set is generated containing the characteristics of single-point cloud data, and it has a good repairing effect on the missing parts of the single data (Luo et al., 2024). Using this fused point cloud to re-build the triangular mesh achieves the transformation from a 3D point cloud model to a 3D surface model. Based on this, by repeating the texture mapping process in the construction of the 3D model using drone oblique photography, a high-precision 3D model based on the fused point cloud data can be obtained (X. Zhou et al., 2024).

3. Results

3.1 3D Modeling of UAV Aerial Survey Data

After extracting feature points and performing image matching on the photogrammetry data, a 3D model meeting the required precision standards is obtained.

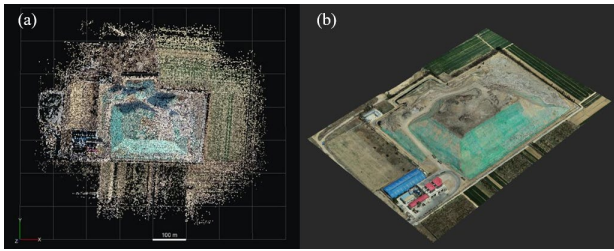


Figure 2. UAV Aerial Point Cloud Result (a), Three-Dimensional Model of Construction Waste Pile (b) During the accuracy evaluation, three samples are taken to calculate the mean as the model point value, which is then compared with the field-measured data. The error calculation

results are as follows. The mean planar error of the 3D model is 0.0194 m, and the mean elevation error is 0.0378 m. Based on the differences between the model measurements and the field-measured verification points, the precision level of this experiment is demonstrated to meet the standards of the UAV CityGML model (Van et al., 2023). Among the 12 verification points, the maximum planar error is 0.0301 m, the minimum is 0.0066 m, the maximum elevation error is 0.0610 m, and the minimum elevation error is 0.0004 m. Both the smallest planar error and the smallest elevation error are at the ground control point 4 (GCP 4). Analysis of the results indicates that points with larger planar errors also correspond to larger elevation errors, as seen in 3.

| GCP | X Coordinate | Y Coordinate | Elevation | Modeling Point | X Coordinate | Y Coordinate | Elevation | Error in Plane | Error in Elevation |
|-------|--------------|--------------|-----------|----------------|--------------|---------------|-----------|----------------|--------------------|
| GCP1 | 413429.9290 | 4367439.3400 | 23.3940 | GCP1c | 413429.9163 | 4367439.3417 | 23.3694 | 0.0128 | -0.0246 |
| GCP3 | 413597.3980 | 4367432.7850 | 22.7150 | GCP3c | 413597.4162 | 43674432.7941 | 22.7004 | 0.0204 | -0.0146 |
| GCP4 | 413719.0460 | 4367427.4990 | 22.3940 | GCP4c | 413719.0495 | 4367427.4935 | 22.3936 | 0.0066 | -0.0004 |
| GCP6 | 413822.0860 | 4367528.4070 | 22.6130 | GCP6c | 413822.1156 | 4367528.4073 | 22.6647 | 0.0296 | 0.0517 |
| GCP7 | 413831.1790 | 4367636.0260 | 22.7340 | GCP7c | 413831.1906 | 4367636.0537 | 22.7135 | 0.0301 | -0.0205 |
| GCP8 | 413489.6560 | 4367441.2720 | 23.3560 | GCP8c | 413489.6600 | 4367441.2799 | 23.3125 | 0.0089 | -0.0435 |
| GCP9 | 413531.6340 | 4367444.7350 | 26.3950 | GCP9c | 413531.6346 | 4367444.7602 | 26.3553 | 0.0252 | -0.0397 |
| GCP11 | 413509.9980 | 4367648.1920 | 23.0790 | GCP11c | 413509.9800 | 4367648.1856 | 23.1400 | 0.0191 | 0.0610 |
| GCP15 | 413811.9350 | 4367625.1470 | 24.3070 | GCP15c | 413811.9371 | 4367625.1608 | 24.3297 | 0.0140 | 0.0227 |
| GCP16 | 413788.0580 | 4367633.8480 | 24.2150 | GCP16c | 413788.0452 | 4367633.8519 | 24.2423 | 0.0134 | 0.0273 |
| GCP18 | 413541.3920 | 4367596.6090 | 33.3090 | GCP18c | 413541.3788 | 4367596.6068 | 33.3597 | 0.0134 | 0.0507 |
| GCP20 | 413660.5810 | 4367554.8530 | 53.4170 | GCP20c | 413660.5915 | 4367554.8338 | 53.4638 | 0.0219 | 0.0468 |

Table 3. Coarse Matching Point Cloud Error

3.2 3D Modeling of Laser Point Cloud Data

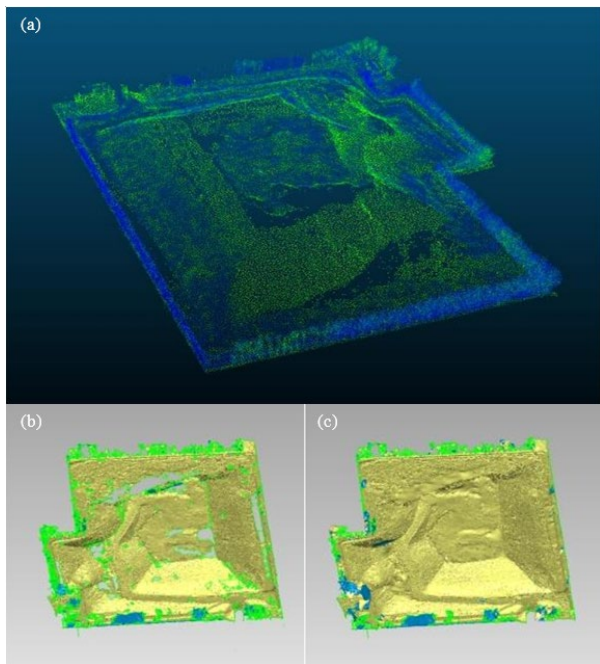


Figure 3. Three-dimensional Point Cloud Downsampling Result (a), Encapsulation Result (b), Gap Filling Result (c)

In the process of obtaining the point cloud of the building debris pile, it is inevitable to have system noise and high point cloud density after trajectory calculation, which affects processing efficiency. Therefore, the point cloud is thinned and clipped to address these issues. After thinning and clipping, the point cloud of the building debris pile is encapsulated. The conversion from point to surface is achieved by constructing a TIN (Triangulated Irregular Network) plane from the point cloud, aiming to restore the three-dimensional morphology of the debris pile as much as

possible. However, due to the presence of blind spots in the monitoring process, there are obvious data gaps in the encapsulated results of the point cloud. Compared to the data voids in drone-based data, the missing data in the three-dimensional point cloud constructed using mobile backpack measurement data is more significant. This method has limitations when applied solely to the construction of three-dimensional models of building debris piles.

3.3 Ground-Aerial Fusion Modeling Based on ICP Point Cloud Fusion

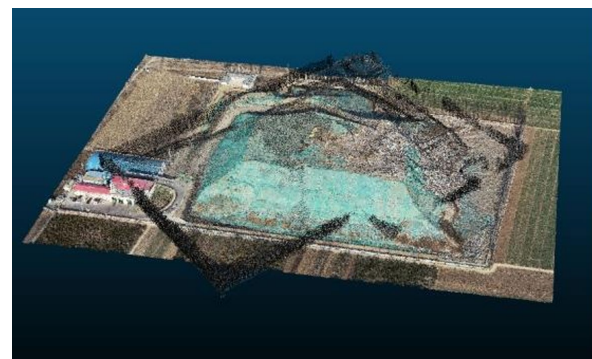


Figure 4. Unfused Point Cloud Overlay Results

In order to unify the fused data in the projected coordinate system, the three-dimensional point cloud generated by drone oblique photography was chosen as the reference, and the SLAM lidar point cloud was fused to achieve the construction of a refined fusion model. The coarse matching of the point clouds used a method involving human-machine interaction, with a total of 4 control points selected. It can be visually observed from the data before fusion that there are significant discrepancies between the two different data sources of point clouds. The coarse matching of the point cloud yielded an RMS deviation of 1.12 meters, indicating a significant offset in the

point cloud. Subsequently, the ICP algorithm was used for iterative point cloud registration. Through the point cloud matching algorithm, the laser point cloud was transformed from the system coordinate system to the projected coordinate system. To validate the point cloud matching effect, nearest neighbor point cloud subtraction was performed to obtain the point cloud distance distribution, showing good alignment results for the debris pile. After registering the point cloud, the merged result effectively mitigated the data gaps caused by blind spots compared to the original, unmerged lidar point cloud. When compared with aerial survey data, the fused data exhibited richer details. For example, details such as dust-proof netting around the debris pile, which might be missing in the 3D reconstruction from drone aerial survey data, were well captured by the SLAM lidar measurement system point cloud data. The fused data successfully inherited these finer details.

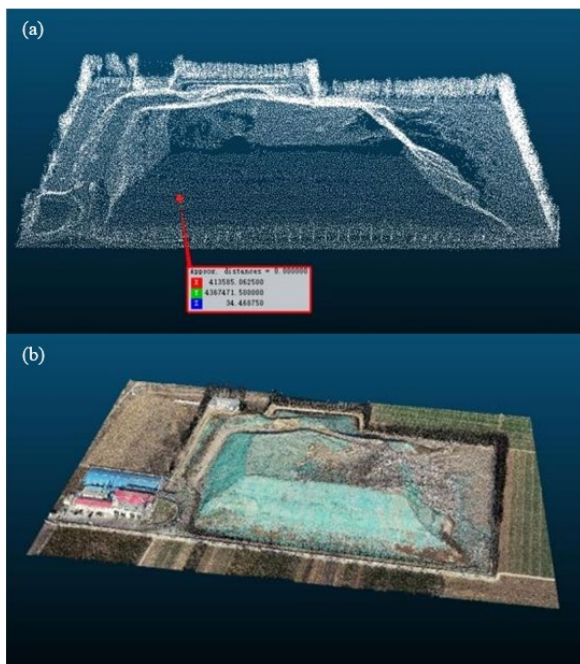


Figure 5. Laser Point Cloud with Completed Matching Calibration (a), Comparison Chart of Point Cloud Fusion Results (b)

3.4 3D Reconstruction and Accuracy Verification Based on Fused Point Cloud

The registered point cloud data is re-imported into the original oblique photogrammetry modelling project. For the layering phenomenon between different point clouds, manually selected connection points are used to address this issue. Since SLAM laser point clouds lack spectral information, connection points are not chosen based on texture information but rather on easily distinguishable corner points, such as wall edges.

Comparison with the three-dimensional model generated from drone oblique photography shows significant improvement in the data void phenomenon in the fused three-dimensional model within the same area. The fused model exhibits richer details. As shown in Figure 6, (a) represents the original image of the bottom of the tree in the three-dimensional model from drone oblique photography, while (b) represents the improved result of data voids in the fused model. The details that were overlooked in the geographical reconstruction of aerial survey data are perfectly restored. The results indicate that the major changes in

the entire model are mainly concentrated at the bottom of the debris pile and the surrounding trees near the wall.

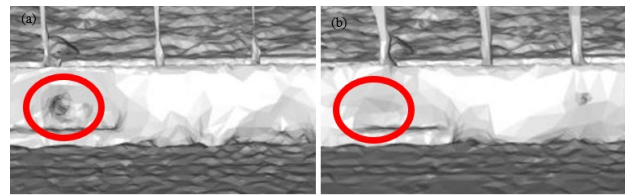


Figure 6. The Original Image (a), the improved result (b)

The accuracy validation of the model was performed using the accuracy validation points used during the fusion process. The validation results showed a planar mean error of 1.87 cm and an elevation mean error of 3.68 cm in the fused model, which meets the corresponding model accuracy requirements. The model constructed based on the fused point cloud data can fully overcome the issue of incompleteness in the three-dimensional model based on a single data source. It also effectively solves the problem of the SLAM mobile measurement system generating point cloud models without projected coordinates. The fused model more accurately captures the features of the debris pile and exhibits richer details. This provides more effective data support for debris monitoring.

4. Discussion and Conclusion

Oblique photogrammetry using drones, as a common method for 3D reconstruction, has been combined with other data sources to achieve refined 3D model reconstruction in many fields (Domingo et al., 2024). Currently, there are few instances of combining drone oblique photogrammetry with multiple data sources for 3D modelling of construction waste. This paper proposes combining drone oblique photogrammetry with LiDAR point cloud data, and through practical verification, the model accuracy shows a significant improvement compared to using a single data source.

Drone oblique photogrammetry has been widely applied in various fields. The data accuracy obtained in this paper meets the relevant specifications and is consistent with the data from drone oblique photogrammetry models in various fields (Cheng et al., 2022). By introducing point cloud data, the accuracy is significantly improved compared to using a single data source. The accuracy of this study is at the same level as the planar accuracy of 3D modelling of railway bridges reported by (Li et al., 2023), with both achieving an accuracy of around 1.9 cm. Compared to the drone oblique photogrammetry model (Li et al., 2018), the planar accuracy of this model is improved by 3.6%, and the elevation accuracy is improved by 2.6%. Compared to using only cyclic drone images, the method proposed in this paper improves the planar accuracy of 3D modelling by 53.25% and the elevation accuracy by 71.69%.

Because the ground control points (GCP) and test points used in this paper are all located on a surface that has not been displaced, after introducing the ICP algorithm and manually partitioning the point cloud, we ensure accurate identification of construction waste in areas with poor data integrity. Compared to the church modelling by (Luhmann et al., 2020), which used only two types of data fusion, the planar error increased by 0.113 cm, and the elevation error increased by 0.134 cm. Compared to single-source 3D modelling of construction waste, the model constructed based on fused point cloud data can fully address the incompleteness issues present in single-source 3D models and effectively resolve the problem of lacking projection coordinates

when generating point cloud models using SLAM mobile measurement systems. This method can more realistically restore the features of the piles, providing richer details and more effective data support for pile monitoring.

The refined 3D model constructed in this paper has some texture loss due to the inclusion of color information in the drone oblique photogrammetry data, while the SLAM LiDAR point cloud does not have color information. If higher requirements for texture information are needed, it is recommended to replace the SLAM LiDAR point cloud data with colored point cloud data obtained from other ground point cloud measurement methods for fusion. It is suggested to use more GCPs when constructing the drone reference model and to add more connecting points after incorporating SLAM data to produce a more accurate model.

References

- Chen, J., Zhao, D., Zheng, Z., Xu, C., Pang, Y., & Zeng, Y. 2024. A clustering-based automatic registration of UAV and terrestrial LiDAR forest point clouds. *Computers and Electronics in Agriculture*, 217, 108648.
- Cheng, M.-L., Matsuoaka, M., Liu, W., & Yamazaki, F. 2022. Near-real-time gradually expanding 3D land surface reconstruction in disaster areas by sequential drone imagery. *Automation in Construction*, 135, 104105.
- Domingo, N., Edirisinghe, H. M., Kahandawa, R., & Wedawatta, G. 2024. Generalised Linear Modelling for Construction Waste Estimation in Residential Projects: Case Study in New Zealand. *Sustainability*, 16(5), 1941.
- Forcael, E., Román, O., Stuardo, H., Herrera, R. F., & Soto-Muñoz, J. 2023. Evaluation of Fissures and Cracks in Bridges by Applying Digital Image Capture Techniques Using an Unmanned Aerial Vehicle. *Drones*, 8(1), 8.
- Guerra, B. C., & Leite, F. 2021. Circular economy in the construction industry: An overview of United States stakeholders' awareness, major challenges, and enablers. *Resources, conservation and recycling*, 170, 105617.
- He, T., Chen, K., Jazizadeh, F., & Reichard, G. 2024. Unmanned aerial vehicle-based as-built surveys of buildings. *Automation in Construction*, 161, 105323.
- Jo, Y. H., Kim, Y. H., & Lee, H. S. 2024. Three-dimensional deviation analysis and digital visualization of shape change before and after conservation treatment of historic kiln site. *Heritage Science*, 12(1), 76.
- Li, G., Liu, J., & Giordano, A. 2022. Robust optimization of construction waste disposal facility location considering uncertain factors. *Journal of Cleaner Production*, 353, 131455.
- Li, J., Peng, Y., Tang, Z., & Li, Z. 2023. Three-Dimensional Reconstruction of Railway Bridges Based on Unmanned Aerial Vehicle–Terrestrial Laser Scanner Point Cloud Fusion. *Buildings*, 13(11), 2841.
- Li, J., Yao, Y., Duan, P., Chen, Y., Li, S., & Zhang, C. 2018. Studies on three-dimensional (3D) modeling of UAV oblique imagery with the aid of loop-shooting. *ISPRS international journal of geo-information*, 7(9), 356.
- Liang, C., Chen, H., Li, R., Chi, W., Wang, S., Hou, S., Gao, Y., & Zhang, P. 2024. Effect of additional water content and adding methods on the performance of recycled aggregate concrete. *Construction and Building Materials*, 423, 135868.
- Liu, J., Li, Y., & Wang, Z. 2023. The potential for carbon reduction in construction waste sorting: A dynamic simulation. *Energy*, 275, 127477.
- Luhmann, T., Chizhova, M., & Gorkovchuk, D. 2020. Fusion of UAV and terrestrial photogrammetry with laser scanning for 3D reconstruction of historic churches in georgia. *Drones*, 4(3), 53.
- Luo, X.-l., Jiang, N., Li, H.-b., Xiao, H.-x., Chen, X.-z., & Zhou, J.-w. 2024. A high-precision modeling and error analysis method for mountainous and canyon areas based on TLS and UAV photogrammetry. *IEEE Journal of Selected Topics in Applied Earth Observations and Remote Sensing*.
- Onososen, A. O., Musonda, I., Onatayo, D., Tjebane, M. M., Saka, A. B., & Fagbenro, R. K. 2023. Impediments to construction site digitalisation using Unmanned Aerial Vehicles (UAVs). *Drones*, 7(1), 45.
- Parente, L., Chandler, J. H., & Dixon, N. 2021. Automated registration of SfM-MVS multitemporal datasets using terrestrial and oblique aerial images. *The Photogrammetric Record*, 36(173), 12-35.
- Petrović, E. K., & Thomas, C. A. 2024. Global Patterns in Construction and Demolition Waste (C&DW) Research: A Bibliometric Analysis Using VOSviewer. *Sustainability*, 16(4), 1561.
- Segara, S., Li, Q. J., Gallotta, A., Wang, Y., Gosling, J., & Rezgui, Y. 2024. A taxonomy of circularity indicators for the built environment: Integrating circularity through the Royal Institute of British architects (RIBA) plan of work. *Journal of Cleaner Production*, 141429.
- Sirimewan, D., Bazli, M., Raman, S., Mohandes, S. R., Kineber, A. F., & Arashpour, M. 2024. Deep learning-based models for environmental management: Recognizing construction, renovation, and demolition waste in-the-wild. *Journal of Environmental Management*, 351, 119908.
- Sivashanmugam, S., Rodriguez, S., Rahimian, F. P., Elghaish, F., & Dawood, N. 2023. Enhancing information standards for automated construction waste quantification and classification. *Automation in Construction*, 152, 104898.
- Terryn, L., Calders, K., Bartholomeus, H., Bartolo, R. E., Brede, B., D'hont, B., Disney, M., Herold, M., Lau, A., & Shenkin, A. 2022. Quantifying tropical forest structure through terrestrial and UAV laser scanning fusion in Australian rainforests. *Remote Sensing of Environment*, 271, 112912.
- Tysiac, P., Sieńska, A., Tarnowska, M., Kedziorski, P., & Jagoda, M. 2023. Combination of terrestrial laser scanning and UAV photogrammetry for 3D modelling and degradation assessment of heritage building based on a lighting analysis: case study—St. Adalbert Church in Gdansk, Poland. *Heritage Science*, 11(1), 53.
- Van, C. L., Cao, C. X., Nguyen, A. N., Pham, C. V., & Nguyen, L. Q. 2023. Building 3D CityGML models of mining industrial structures using integrated UAV and TLS point clouds. *International Journal of Coal Science & Technology*, 10(1), 69.

Wang, Z., Hu, T., & Liu, J. 2024. Decoupling economic growth from construction waste generation: Comparative analysis between the EU and China. *Journal of Environmental Management*, 353, 120144.

Zeng, He, & Zhang. 2023, 2023-03-25. City-level high-precision modeling technology integrating laser point cloud. *Bulletin of Surveying and Mapping*, 0(3), 133-138.

Zhao, Y., Zhu, Z., Liu, W., Zhan, J., & Wu, D. 2023. Application of 3D laser scanning on NATM tunnel deformation measurement during construction. *Acta Geotechnica*, 18(1), 483-494.

Zhou, J.-w., Jiang, N., & Li, H.-b. 2024. Automatic discontinuity identification and quantitative monitoring of unstable blocks using terrestrial laser scanning in large landslide during emergency disposal. *Landslides*, 21(3), 607-620.

Zhou, X., Zhu, Q., Zhang, Q., & Du, Y. 2024. The full-field displacement intelligent measurement of retaining structures using UAV and 3D reconstruction. *Measurement*, 114311.